Available online at www.sciencedirect.com
SCIENCE DIRECT®
ELSEVIER
Journal of Magnetism and Magnetic Materials 300 (2006) 436–444
Journal of magnetism and magnetic materials
www.elsevier.com/locate/jmmm

MOKE hysteresis loop method of determining the anisotropy constants of ferromagnetic thin films: fe on GaAs(1 0 0) with overlayers of Au and Cr

N.A. Morley[a,*], M.R.J. Gibbs[a], E Ahmad[b], I Will[b], Y.B. Xu[b]

[a]*Department of Engineering Materials, University of Sheffield, Sheffield, S1 3JD, UK*
[b]*Department of Electronics, University of York, York, YO10 5DD, UK*

Received 21 April 2005; received in revised form 23 May 2005
Available online 22 June 2005

Abstract

This paper presents a quantitative method used to determine the magnetocrystalline anisotropy constants of thin magnetic films from normalized magnetization data measured on a magneto-optic Kerr effect (MOKE) magnetometer. The method is based on a total magnetic energy density model, and incorporates higher order effects in the detected signal. By way of illustration, the method is used to determine the magnetocrystalline anisotropy constants of epitaxial thin Fe films on GaAs substrates, which have different overlayers. It is shown that a Cr overlayer on a 30 ML thick Fe film reduces the uniaxial contribution to the magnetic anisotropy compared with an Au overlayer.

PACS: 75.70.-i; 75.70.Ak; 75.30.Gw; 75.40.Mg

Keywords: Fe/GaAs films; Anisotropy; MOKE magnetometry

1. Introduction

One method used to determine the normalized magnetization loop of a magnetic film is the magneto-optic Kerr effect (MOKE) magnetometer [1–3]. MOKE magnetometers provide data that can be presented in the form of the normalized magnetization loop, by using a laser beam which is reflected off the surface of the film into a photodetector. The laser is p-polarized using a polarizer before being incident on the film, which means the electric field of the laser is parallel to the plane of incidence. After the sample, the reflected beam passes through an analyzer before the photodetector. The film is in a uniform magnetic

*Corresponding author. Fax: +440 1142728079.
E-mail address: n.a.morley@sheffield.ac.uk (N.A. Morley).

0304-8853/$ - see front matter © 2005 Elsevier B.V. All rights reserved.
doi:10.1016/j.jmmm.2005.05.034

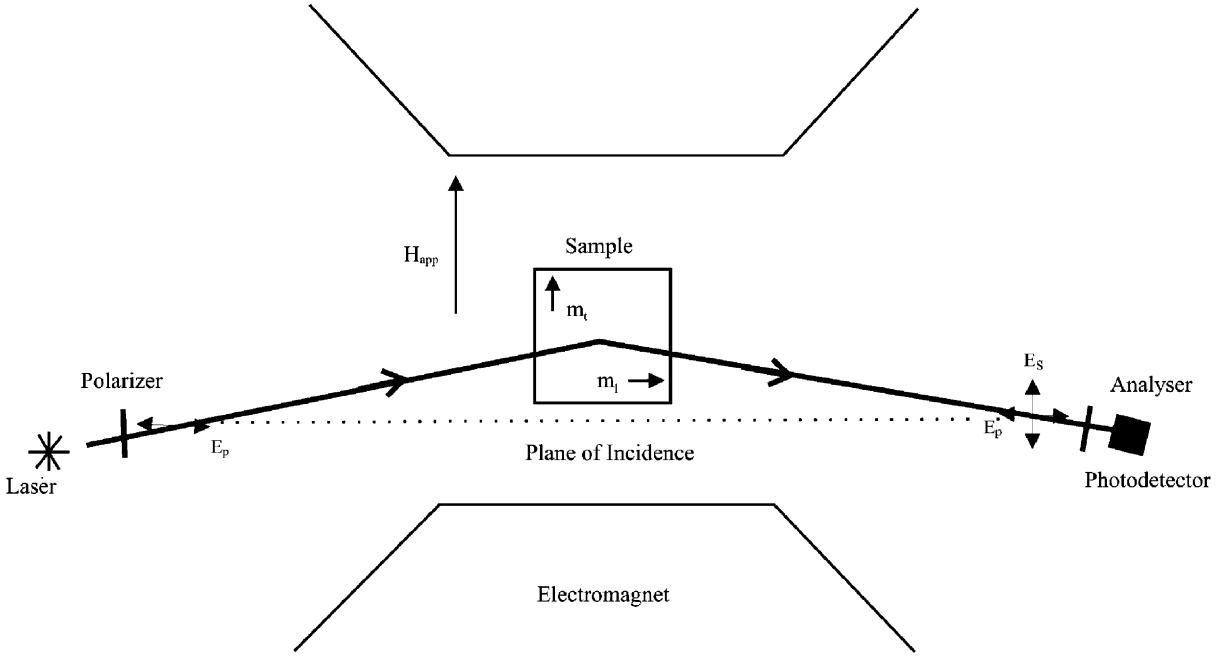

Fig. 1. Schematic diagram of the MOKE magnetometer, which shows the plane of incidence of the laser beam with respect to the longitudinal (m_l) and transverse (m_t) magnetizations of the film and the applied field (H_a) direction.

field, which is perpendicular to the plane of incidence of the laser (transverse MOKE geometry) (Fig. 1). The advantages of MOKE magnetometers are they are simple, non-destructive, room temperature instruments. The normalized magnetization loops measured on MOKE magnetometers are generally used as qualitative data. In this paper we present a method based on a total energy density model, which uses the magnetization data to determine quantitative information on the magnetic anisotropies in the film.

Florczak et al. [4,5] showed that the output voltage of the photodetector in a MOKE magnetometer is a function of the angle between the plane of incidence and the analyzer pass plane θ_a (Fig. 1). Hence the measured hysteresis loop changed shape as this angle increased from 0° to 90°. For the MOKE magnetometer, the normalized intensity, I/I_o, at the photodetector is given by [5]

$$\frac{I}{I_o} = \left|\frac{E_r}{E_o}\right|^2, \tag{1}$$

where E_r/E_o is the normalized reflected electric field of the laser. The reflected electric field will contain both p- and *s*-polarized components. From previous work the reflected field is given by [5]

$$E_r = E_o\left[\left(m_t^2 r_{pp}^t + m_l^2 r_{pp}^l\right)\cos\theta_p\cos\theta_a + m_l^2 r_{ps}^l \sin\left(\theta_p - \theta_a\right) + r_{ss}^l \sin\theta_p \sin\theta_a\right] \tag{2}$$

where m_t and m_l are the transverse and longitudinal magnetizations (Fig. 1). The angles θ_p and θ_a are the angles between the plane of incidence and the transmission axis of the polarizer and analyzer, respectively. The terms r_{pp}^l, r_{pp}^t, r_{ps}^l and r_{ss}^l are the complex Fresnel coefficients for light reflected from a magnetic film [6–8]. The superscript l and t represent the longitudinal and transverse components, respectively. The subscript p and s represent the polarized light being parallel (p-polarized) and perpendicular (s-polarized) to the plane of incidence. Hence the intensity measured at the photodetector is

determined by substituting Eq. (2) into Eq. (1), and is given by [5]

$$\begin{aligned}\frac{I}{I_o} = &\left[\left|m_l^2 r_{pp}^l + m_t^2 r_{pp}^t\right|^2 \cos^2\theta_p \cos^2\theta_a \right.\\ &+ \left|m_l^2 r_{ps}^l\right|^2 \sin^2(\theta_p - \theta_a) + \left|r_{ss}^l\right|^2 \sin^2\theta_p \sin^2\theta_a\\ &+ \left[\left(m_l^2 r_{pp}^l + m_t^2 r_{pp}^t\right) m_l^2 r_{ps}^l + \text{cc}\right]\\ &\times \cos\theta_p \cos\theta_a \sin(\theta_p - \theta_a)\\ &+ \left[\left(m_l^2 r_{pp}^l + m_t^2 r_{pp}^t\right) r_{ss}^{l*} + \text{cc}\right]\\ &\times \cos\theta_p \cos\theta_a \sin\theta_p \sin\theta_a\\ &\left.+ \left[r_{ss}^l m_l^2 r_{ps}^{l*} + \text{cc}\right] \sin\theta_p \sin\theta_a \sin(\theta_p - \theta_a)\right],\end{aligned} \tag{3}$$

where cc is the complex conjugate of the expression and * represents the complex conjugate of the Fresnel coefficient. For the experiments carried out in this paper, the polarizer angle was parallel to the plane of incidence, $\theta_p = 0^\circ$, so that the laser was p-polaried. Hence the longitudinal and transverse magnetizations were measured. Thus substituting this angle into Eq. (3), the normalized intensity of the photodetector becomes [5]

$$\begin{aligned}\frac{I}{I_0} = &\left|m_t^2 r_{pp}^t + m_l^2 r_{pp}^l\right|^2 \cos^2\theta_a + \left|m_l^2 r_{ps}^l\right|^2 \sin^2(\theta_a)\\ &- \left[\left(m_t^2 r_{pp}^t + m_l^2 r_{pp}^l\right) m_l^2 r_{ps}^{l*} + \text{cc}\right] \cos\theta_a \sin\theta_a.\end{aligned} \tag{4}$$

The transverse and longitudinal magnetizations are taken to be $m_t = m_s \sin(\varphi + \pi/2)$ and $m_l = m_s \cos(\varphi + \pi/2)$, where φ is the angle between the magnetization and the applied field. Thus the longitudinal magnetization is parallel to the plane of incidence of the laser. Florczak simplified Eq. (4) by assuming the analyzer angle was not close to 90° with respect to the pass plane of the polarizer [4], i.e. the $\sin^2\theta_a$ was neglected.

For the more sensitive MOKE magnetometer measurements we carry out, the analyzer angle is close to extinction, ($85^\circ < \theta_a < 90^\circ$), thus all the terms have to be included in Eq. (4). By substituting the magnetization components into Eq. (4), and collecting all the constants together, the intensity is written in terms of the angle between the magnetization and the applied field, and is given by

$$\begin{aligned}\frac{I}{I_o} = &A\cos^2\theta_a + \left(B\cos^2\theta_a\right)\cos\varphi\\ &+ \left(C\sin\theta_a\cos\theta_a\right)\sin\varphi + \left(D\sin^2\theta_a\right)\sin^2\varphi,\end{aligned} \tag{5}$$

where A, B, C and D are constants which depend on the index of refraction of Fe, the magneto-optic constant, and the angle of incidence of the laser beam on the film. The constants A, B, and C are derived by Florczak [4], and are given in the appendix of this paper. The constant D is derived for this paper in the appendix. When the analyzer angle is set between 0° and 85°, the measured magnetization loops are symmetric with respect to the field, as the $B\cos^2\theta_a$ and $C\sin\theta_a\cos\theta_a$ terms are larger than the $D\sin^2\theta_a$ term; hence the $D\sin^2\theta_a$ term is ignored. Thus the measured magnetization loop is only a function of the first-order terms in φ. While when the analyzer angle is set close to 90°, the measured magnetization loops are asymmetric with respect to the field (Fig. 4), due to the $D\sin^2\theta_a$ term being the same order of magnitude as the other two constant terms. Hence the new overall expression (Eq. (5)) now includes the second-order term, $\sin^2\varphi$. This introduces asymmetry into the loop.

The study of epitaxial Fe on GaAs(1 0 0) substrates is of great interest, due to the unexpected uniaxial anisotropy which appears for thicknesses of Fe less than 100 ML. The origin of this uniaxial anisotropy is thought to be due to the Fe–GaAs(1 0 0) interface [9]. Previous work has suggested that the presence of $Fe_3Ga_{2-x}As_x$ [10] or dangling bonds of GaAs [11] at the interface or the strain due to the lattice mismatch [12] could be the cause. In order to consider the anisotropic properties of the films, and relate these to crystallographic directions within the Fe film, the crystallographic orientation of the GaAs wafers used for film growth must be established (Fig. 2). It is widely accepted that Fe grows epitaxially on GaAs(1 0 0) according to Fe(1 0 0)<001> ||GaAs(1 0 0)<001> [13], thus Fig. 2 is also indicative of the crystallographic directions in the Fe film after deposition.

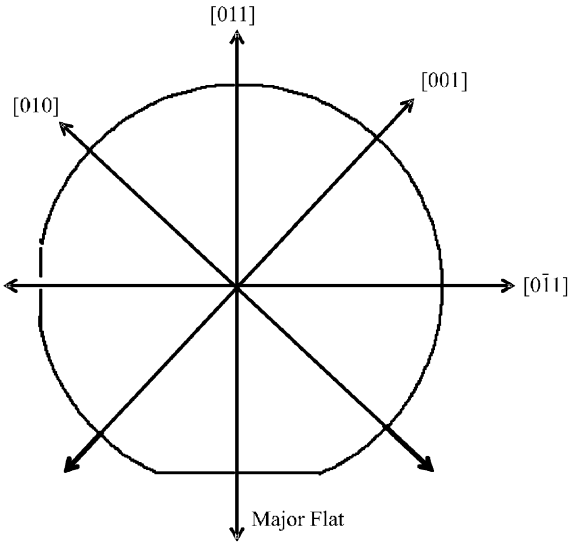

Fig. 2. The crystallographic orientation of the GaAs wafers used as substrates for the subsequent deposition of Fe films.

For Fe films thinner than 10 ML, only uniaxial anisotropy is observed, with the hard axis along the [0 $\bar{1}$ 1] direction and the easy axis along the [0 1 1] direction [9,11] (Fig. 3a). For Fe thicker than 100 ML only cubic anisotropy is observed in the magnetization process, with the hard axes along the [0 1 1] directions, and the easy direction along [0 0 1] (Fig. 3b). Hence between these thicknesses of Fe, mixed cubic and uniaxial anisotropy is observed, with the hard-hard axis along the [0 $\bar{1}$ 1] direction, the hard-easy axis along the [0 1 1] direction, and the easy axes between the [0 0 1] and [0 1 1] directions (Fig. 3c).

We shall assume, as have others, that the magnetization process proceeds by pure and coherent rotation of the magnetization vector in the film plane under the influence of an external in-plane applied field [11,14,15]. The total magnetic energy density (F) in the plane of a thin Fe film in the most general case may be written in terms of the magnetocrystalline and uniaxial anisotropies and the Zeeman energy density. In general, F is given by

$$F = K_1(t)\left(\alpha_1^2\alpha_2^2 + \alpha_1^2\alpha_3^2 + \alpha_2^2\alpha_3^2\right) + K_2(t)\left(\alpha_1^2\alpha_2^2\alpha_3^2\right) + K_u(t)\sin^2(\theta) - HM\cos\varphi \quad (6)$$

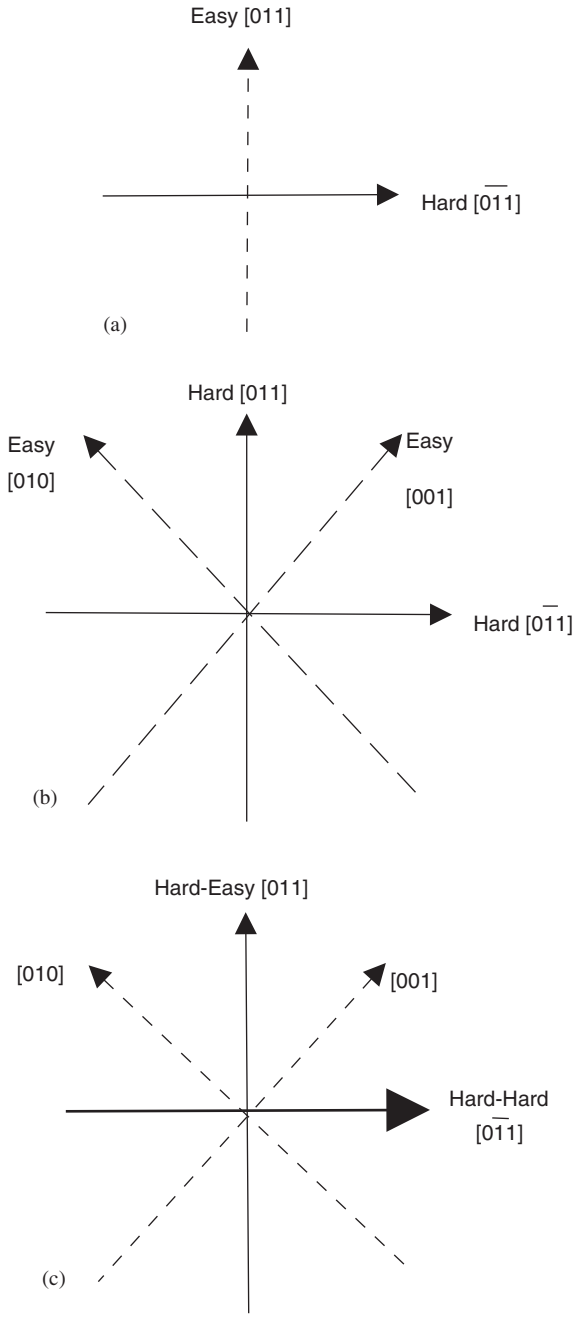

Fig. 3. For a thin iron film the direction of the anisotropic energy axes, when the anisotropy is (a) uniaxial, (b) cubic and (c) both. The easy axes are represented by the dashed lines and the hard axes represented by the solid lines.

where $K_1(t)$ and $K_2(t)$ are the cubic magnetocrystalline anisotropy constants, $K_u(t)$ is the uniaxial anisotropy constant, θ is the angle between the magnetic field and the uniaxial anisotropy easy direction in the film and φ is the angle between the magnetic field (H) and the in-plane magnetization (M). The α_i are the direction cosines of the magnetization with respect to the crystallographic axes in the Fe film. The second order cubic magnetocrystalline anisotropy constant, $K_2(t)$, is not involved any further as the geometry puts this contribution to zero. Both remaining anisotropy constants may be functions of the Fe layer thickness, t. Taking account of the film crystallography, and the geometry to be used in the measurement (i.e. the field is applied along the [0 $\bar{1}$ 1] direction), Eq. (6) becomes

$$F = \frac{1}{4}K_1(t)\sin^2\left(2\varphi - \frac{\pi}{2}\right) + K_u(t)\sin^2\left(\frac{\pi}{2} - \varphi\right) - HM\cos\varphi \quad (7)$$

Eq. (7) can only be used for magnetic rotation in the single domain state and may not apply in a multi-domain state. For any applied field, the magnetization will lie along the (local) direction of minimum energy density in the film, i.e. where $dF/d\varphi = 0$. As the hard axes have different energy densities it is possible to observe two Barkhausen jumps in the measured magnetization [15–17]. This is because for some field directions with respect to the [0 0 1] axis, it is more energetically favourable for the magnetization to jump over the two hard axes separately, than together.

Generally the anisotropy constants of a magnetic film have been determined using Brillouin light scattering (BLS) [11,18,19] or ferromagnetic resonance (FMR) [20–22]. Mattheis et al. [23], presented a method, which determined the uniaxial anisotropy constant using a MOKE magnetometer with a rotating field. The disadvantage of this method was it could only be used for uniaxial anisotropy. We have developed the MOKE fitting method, which determines the anisotropy constants from the normalized magnetization loop, when the analyzer angle is close to extinction. This fitting method convolutes the intensity output of the photodetector (Eq. (5)) with the magnetization loop along the [0 $\bar{1}$ 1] direction, (Eq. (7)). To start, the angle φ is calculated using a Maple™ programme, which solves the differential of Eq. (7) with respect to φ, for initial estimates of the anisotropy constants. These estimates are either taken from literature values, or known properties of the material in bulk form. The saturation magnetization is determined by measuring the films on a vibrating sample magnetometer (VSM). The φ values are then put into Eq. (5), with the known constants A, B, C, D and the angle of the analyzer. The theoretical magnetization loop is then normalized and compared with the measured MOKE loop. The values of K_1 and K_u are varied iteratively until the error between the experimental and theory data is a minimum. The best fit values are taken as giving the anisotropy constants for the film. To demonstrate the validity of this MOKE fitting method, the anisotropy constants for two 30 ML Fe films on GaAs(1 0 0) substrate with different overlayers are presented here. We have published elsewhere data using this technique for a range of thin film magnetic configurations [24].

2. Experimental set-up

From the previous section, the arrangement of the MOKE magnetometer is important, as it determines the output voltage of the photodetector. For the data presented in this paper, the polarizer angle was set so that the laser was p-polarized and the angle of the pass plane of the analyzer was set at 88° with respect to the pass plane of the polarizer. This gave high sensitivity when measuring the magnetization changes of the thin films.

The two thin Fe on GaAs(1 0 0) substrate films measured in this paper were grown using molecular beam epitaxy (MBE), at York University [14]. The GaAs(1 0 0) substrates were purchased from Wafer Technology Ltd., with the major flat parallel to the [0 $\bar{1}$ $\bar{1}$] crystallographic direction. Prior to film deposition, they were etched using an etchant, comprising H_2SO_4 (sulphuric acid):H_2O_2 (hydrogen peroxide):H_2O (de-ionized water) at a ratio of 4:1:1, followed by de-ionized water rinsing and dehydrating using iso-propyl alcohol (IPA). They were then placed into the MBE system, and were

cleaned using ion sputter at 200 °C for 20 min. The substrates were then annealed at 550 °C for 45 min, and then allowed to cool. The surface flatness and reconstruction of the GaAs(1 0 0) substrates were determined using reflection high energy electron density (RHEED). The Fe films were then grown at 50 °C and 1×10^{-10} mbar. The growth rate was kept constant, by ensuring the emission current between the filament and the source material was constant. Epitaxial growth occurs when the growth rate is 1 ML min^{-1}. For the Fe film, the flatness and the uniformity along the [0 1 1] direction was checked using RHEED. The patterns showed epitaxy on GaAs(1 0 0) with the relationship Fe(1 0 0)<0 0 1>||GaAs(1 0 0)<0 0 1>. The evaporation procedure was then repeated for the overlayer material. For both films, the Fe thickness was 30 ML. For film 1, the Fe layer was capped with 20 ML of Au, while for film 2 the Fe layer was capped with 15 ML of Cr.

3. Results

The two 30 ML Fe films were measured using a MOKE magnetometer, with the field perpendicular to the plane of incidence (Fig. 1). The normalized magnetization loops were measured for the [0 1 1] direction and the [0 $\bar{1}$ 1] direction (Fig. 4). For each film, the magnetocrystalline anisotropy constants were determined using the method described in this paper. The saturation magnetisation was determined using a VSM to be $\mu_o M_s = 2.1$ T, which is the bulk Fe value. The fitted magnetization loops are plotted on top of the measured magnetization loops. film 1 (Fig. 4(a)), it can be seen that the magnetization process in the [0 $\bar{1}$ 1] direction is different to the magnetization process in the [0 1 1]. This is best interpreted as the film containing cubic and uniaxial anisotropy [9,25]. From the fitting procedure the values of the anisotropy constants are $K_1 = 32000 \pm 2500$ J m^{-3} and $K_u = 29000 \pm 2300$ J m^{-3}. For film 2 (Fig. 4(b)), the magnetization process along the [0 1 1] direction is the same as the magnetization process along the [0 $\bar{1}$ 1] direction, hence cubic anisotropy dominates over any uniaxial anisotropy. From the fitting procedure, the values of the anisotropy constants are: $K_1 = 22000 \pm 550$ J m^{-3} and $K_u = 9000 \pm 225$ J m^{-3}. This means the Cr overlayer has reduced the uniaxial anisotropy contribution in the Fe film, in comparison to the Au overlayer.

4. Discussion

The method presented in this paper provides, a way of determining the anisotropy constants from normalized magnetization data. Other researchers have resorted to such techniques as Brillouin light scattering (BLS) [11,18,19]. The asymmetry with respect to the field observed in the measured magnetization loops due to the photodetector output has been resolved by fitting Eq. (5) to the data, which incorporates the effect of the relative angle between the plane of incidence and the pass plane of the analyzer (Fig. 1). This method is also useful for films which contain more than one magnetocrystalline anisotropy, such as cubic and uniaxial, as it does not rely on the ratio of the combined anisotropy constants to the magnetization.

The error on the calculated anisotropy constants is dependant on the error on the angles of the polarizer and analyzer, and the signal to noise ratio of the normalized magnetization data. The error on the polarizer and analyzer angles affects the weighting between the first and second-order φ terms in Eq. (5). The polarizer angle was set to ensure that the laser was p-polarized. Thus if the error on the polarizer angle less than 5° from $\theta_p = 0°$, then the assumptions made to attain Eq. (4) were not affected. If the polarizer angle was larger than this, then the weighting of the terms in Eq. (5) would be affected and an additional offset term would have to be included. It is extremely improbable that the polarizer angle was out by more than 5°, due to the care taken in setting up the MOKE magnetometer; hence the assumptions made to attain Eq. (5) are valid.

An error is more likely to have occurred when measuring the analyzer angle, as the error was $\Delta\theta_a = \pm 1°$. This change of 1° can vary the weighting of each term in Eq. (5). In Table 1, the variation in the value of each trigonometric term in Eq. (5) is given for angles close to 90°. It is

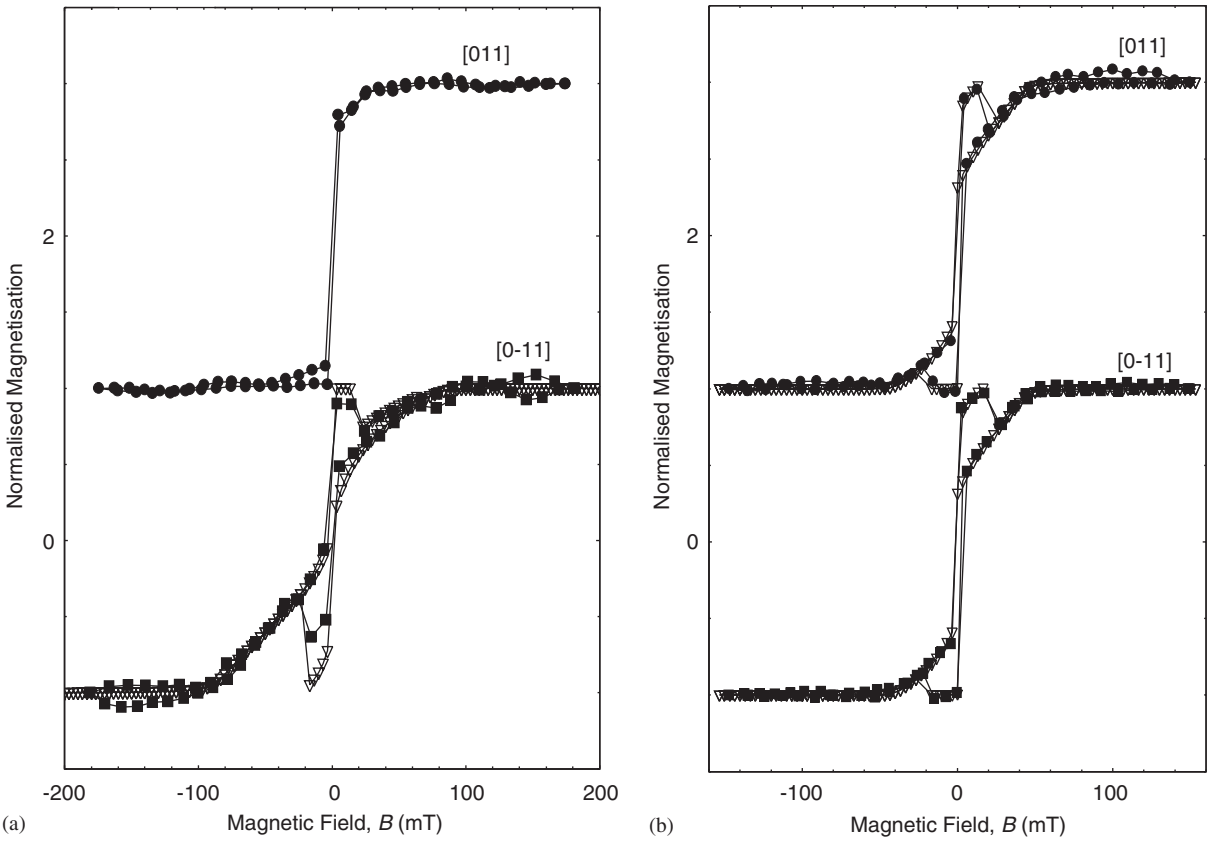

Fig. 4. Normalized magnetization of (a) Au/30 ML Fe/GaAs film and (b) Cr/30 ML Fe/GaAs film, as a function of applied magnetic field, for the field along the $[0\,\bar{1}\,1]$ and the $[0\,1\,1]$ direction, for both experimental data (filled shapes) and theory data (open shapes).

observed that there is a significant change in the values of $\cos^2\theta_a$ and $\sin\theta_a\cos\theta_a$ for the small change in angle, while there is no change in the $\sin^2\theta_a$ term. Hence for a small change in the analyser angle, the magnitudes of the first order φ term constants ($B\cos^2\theta_a$ and $C\sin\theta_a\cos\theta_a$) in Eq. (5) vary strongly, compared to the second order φ term constant ($D\sin^2\theta_a$). The analyzer angle was taken from the experimental set-up, and was directly used in the fitting method, to determine the anisotropy constants. To ensure that the correct angle value was used, θ_a was a free parameter during the fitting method. In no instance did the fitted parameter vary by more than 1° from the nominally set value. Hence the error due to any uncertainty in the analyzer angle was reduced by this step. In conclusion, the weighting between the first order φ term constants ($B\cos^2\theta_a$ and $C\sin\theta_a\cos\theta_a$) and second order φ term constant ($D\sin^2\theta_a$) does vary with the analyzer angle, but during the fitting procedure, the actual value of the angle was checked; therefore reducing the error on the calculated anisotropy constants.

Table 1
Variation in the analyzer angle terms in Eq. (5), if the angle is changed by 1°

Angle (θ_a)	$\sin\theta_a$	$\cos\theta_a$	$\sin^2\theta_a$	$\cos^2\theta_a$	$\sin\theta_a\cos\theta_a$
87°	0.998	0.052	0.997	0.0027	0.052
88°	0.999	0.035	0.998	0.0012	0.035
89°	0.999	0.017	0.999	0.0003	0.017

From Fig. 4 and the theoretical data, it is seen that the Cr overlayer has reduced the uniaxial

anisotropy in the Fe film. Previous measurements of 30 ML Fe/GaAs have studied films with overlayers of Au [9,19,26], Si [20] and Cr [11]. Table 2 gives a summary of the cubic and uniaxial anisotropy constants measured for 30 ML of Fe on GaAs substrate from literature. For film 1 (Au overlayer), the values of K_1 and K_u are within the range of values in the literature for Au overlayer Fe/GaAs films. The difference between the values could be due to different reconstructions of the substrates, as Moosbühler showed this affected the anisotropy constants [26]. In this paper the films are 1×1 reconstructions, while the literature films are either 4×6 or 2×4. The surface reconstructions were determined by the established technique of RHEED.

From Gester's paper [11] on Fe/GaAs film, with Cr overlayer, the uniaxial anisotropy constants ranged between 8000 to 24 000 J m^{-3} for Fe thicknesses less than 60 ML. It was suggested in the paper that this was due to the sensitivity of K_u to the growth condition. For films 1 (Au overlayer) and 2 (Cr overlayer) in this paper, the growth temperatures were the same, and the growth rates and hence the thickness were similar. The precise thickness of the two samples may be slightly thicker or thinner than expected ($\pm 10\%$), but they will both vary in the same direction. Thus it is also possible that the growth rate affected the uniaxial anisotropy for the Cr overlayer film, consistent with Gester's conclusion [11]. It remains to be noted that Au capped Fe films on GaAs do not appear to have the same growth rate dependence of anisotropy constants. Other studies of Cr overlayer films have suggested that there is an interaction between the Cr and the Fe at the interface [18,27]. For these measurements, the substrate was Ag(1 0 0), and there was no uniaxial anisotropy present in the film. These are the first measurements to show that the Cr overlayer reduces the uniaxial anisotropy in an epitaxial Fe/GaAs film, so that the magnetocrystalline anisotropy is almost purely cubic. This explanation can also be used for the data presented by Gester [11]. The most probable reason for the reduction in the uniaxial anisotropy is that the Cr intermixes with the Fe at the interface. Intermixing at the interface occurs, when the material being deposited has a larger melting point, than the underlayer material [28]. For the Fe–Cr interface, the melting point of Fe is 1808 K, while the melting point of Cr is 2130 K, thus intermixing will have occurred. While for the Fe–Au interface, the melting point of Au is 1337 K, thus intermixing will not have occurred. Cr alloyed with Fe would also reduce the Fe moment, and may even produce a dead layer [29]. Thus the change in the magnetic properties of the Fe/GaAs films with Cr overlayer is due to the Cr intermixing with the Fe at the interface.

Table 2
Magnetocrystalline anisotropy constants for 30 ML Fe/GaAs for different capping layers

Film	Capping layer	K_1 (J m^{-3})	K_u (J m^{-3})
Film 1	Au	$32\,000 \pm 2500$	$29\,000 \pm 2300$
Film 2	Cr	$22\,000 \pm 550$	9000 ± 225
McPhail[19]	Au	29 700	23 000
Moosbühler[20]	Au	30 600	29 900
Brockmann[4]	Au	32 400	27 500
Zuberek[21]	Si	32 100	—

5. Conclusions

This paper presents a method which determines the magnetocrystalline anisotropy constants from normalized magnetization loops measured on a MOKE magnetometer. The method incorporates the relationship between the photodetector intensity and the angle between the pass plane of the analyzer and the plane of incidence of the laser, with a total magnetic energy density model.

As an example two 30 ML Fe/GaAs films with different overlayers were measured. It was determined using the theory method that the magnetocrystalline anisotropy constants were different for the two films. The Au overlayer film had cubic and uniaxial anisotropy constants which were similar to those in the literature. While the Cr overlayer film showed a strong cubic anisotropy, due to the Cr intermixing with the Fe at the interface, which reduced the uniaxial contribution. Thus the overlayer used for thin Fe/GaAs films is important, as it affects the overall anisotropy of the film.

Appendix

The constants A, B, C and D are derived from the reflection coefficients in Eq. (7). They are function of the magneto-optic constant, Q, the index of refraction, n, and the angle of incidence of the laser, ϕ. The full derviations of A, B and C are found in Florczak's paper [4], thus they are

$$A \equiv \left|\frac{n\beta-\beta'}{n\beta+\beta'}\right|^2,$$

$$B \equiv \left|\frac{n\beta-\beta'}{n\beta+\beta'}\right|^2\left(\frac{in^2\,Q\sin(2\phi)}{n^2(n^2\cos^2\phi-1)+\sin^2\phi}+\mathrm{cc}\right),$$

$$C \equiv \frac{n\beta-\beta'}{n\beta+\beta'}\left(\frac{in^{2*}Q^{*}\beta\sin\phi}{n^{2*}\beta'^{*}\left(n^{*}\beta+\beta'^{*}\right)\left(\beta+n^{*}\beta'^{*}\right)}\right)+\mathrm{cc},$$

where $\beta=\cos\phi$, $\beta'=\left[1-(\sin^2\phi/n)^2\right]^{1/2}$ and cc is the complex conjugate of the expression. From Eq. (7), the constant D is derived from $\left|m_1^2 r_{\mathrm{ps}}^{\mathrm{l}}\right|^2$, thus substituting the Fresnel coefficient $r_{\mathrm{ps}}^{\mathrm{l}}=\frac{i\beta n^2(Q/m_1)\sin\theta}{n^2\beta'(n\beta+\beta')(\beta+n\beta')}$ into D and removing the magnetization term gives

$$D \equiv \left|\frac{inQ\beta\sin\phi}{n^2\beta'\left(n\beta+\beta'\right)\left(\beta+n\beta'\right)}\right|^2.$$

For the thin Fe films in this paper, the constants were taken to be $n=2.88+3.05\mathrm{i}$ [30] and $Q=0.027$ [31], although other values of n and Q are possible [32].

References

[1] P.Q.J. Nederpel, J.W.D. Martens, Rev. Sci. Instrum. 56 (1985) 687.
[2] D.A. Allwood, G. Xiong, M.D. Cooke, et al., J. Phy. D: Appl. Phys. 36 (2003) 2175.
[3] J. Zak, E.R. Moog, C. Liu, et al., J. Magn. Magn. Mater 89 (1990) 107.
[4] J.M. Florczak, E.D. Dahlberg, Phys. Rev. B 44 (1991) 9338.
[5] J.M. Florczak, E. Dan Dahlberg, J. Appl. Phys. 67 (1990) 7520.
[6] M.J. Freiser, IEEE Trans. Mag. MAG-4 (1968) 152.
[7] R.P. Hunt, J. Appl. Phys. 38 (1967) 1652.
[8] E.R. Moog, C. Liu, S.D. Bader, et al., Phys. Rev. B 39 (1989) 6949.
[9] M. Brockmann, M. Zolfl, S. Miethaner, et al., J. Magn. Magn. Mater. 198–199 (1999) 384.
[10] A. Filipe, A. Schuhl, P. Galtier, Appl. Phys. lett. 70 (1996) 129.
[11] M. Gester, C. Daboo, R.J. Hicken, et al., J. Appl. Phys. 80 (1996) 347.
[12] D. Sander, A. Enders, J. Kirschner, J. Magn. Magn. Mater 200 (1999) 439.
[13] Y.B. Xu, IEEE Trans Mag. 35 (1999) 3661.
[14] E. Ahmad, N.A. Morley, I. Will, et al., J. Appl. Phys. 95 (2004) 6555.
[15] C. Daboo, R.J. Hicken, D.E.P. Eley, et al., J. Appl. Phys. 76 (1994) 5586.
[16] N.A. Morley, M.R.J. Gibbs, R. Zuberek, et al., J. Phys. Conden. Matter 16 (2004) 4121.
[17] C. Daboo, R.J. Hicken, E. Gu, et al., Phys. Rev. B 51 (1995) 15964.
[18] R.J. Hicken, S.J. Gray, A. Ercole, et al., Phys. Rev. B 55 (1997) 5898.
[19] S. McPhail, C.M. Gurtler, F. Montaigne, et al., Phys. Rev. B 67 (2003) 1.
[20] R. Zuberek, K. Fronc, A. Szewczyk, et al., J. Magn. Magn. Mater 260 (2003) 386.
[21] T.L. Monchesky, B. Heinrich, R. Urban, et al., Phys. Rev. B 60 (1999) 10242.
[22] J. Pelzl, R. Meckenstock, D. Spoddig, et al., J. Phys. Condens. Matter 15 (2003) S451.
[23] R. Mattheis, G. Quednau, J. Magn. Magn. Mater 205 (1999) 143.
[24] N.A. Morley, M.R.J. Gibbs, E. Ahmad, et al., J. Phys. Condens. Matter 17 (2005) 1201.
[25] Y.B. Xu, D.J. Freeland, M. Tselepi, et al., J. Appl. Phys. 87 (2000) 6110.
[26] R. Moosbuhler, F. Bensch, M. Dumm, et al., J. Appl. Phys. 91 (2002) 8757.
[27] R.J. Hicken, A. Ercole, S.J. Gray, et al., J. Appl Phys. 79 (1996) 4987.
[28] B. Heinrich, J.F. Cochran, D. Venus, et al., J. Appl. Phys. 79 (1996) 4518.
[29] N.A. Morley, S.L. Tang, M.R.J. Gibbs, et al., J. Appl. Phys. 97 (2005) 10H501.
[30] P.B. Johnson, R.W. Christy, Phys. Rev. B 9 (1974) 5060.
[31] J.H. Judy, J.K. Alstad, G. Bate, et al., IEEE Trans. Mag. Mag-4 (1968) 401.
[32] M. Corke, A.W.J. Dawkins, R.B. Inwood, J. Phys. E: Sci Instrum. 15 (1982) 251.